Lobetyolin alleviates IMQ-induced psoriasis-like skin inflammation by maintaining the homeostasis of the skin and inhibiting the inflammatory cytokines in dendritic cells

JIANPING HE[1*], CHENXI FENG[1*], YAOHAN XU[1], SIJI CHEN[1], JIE CHEN[1], JINGYING PAN[1], YINJING SONG[1], HAO CHENG[1], JIANG ZHU[1] and JIE ZHU[2]

[1]Department of Dermatology and Venereology, Sir Run Run Shaw Hospital, Zhejiang University School of Medicine, Hangzhou, Zhejiang 310016, P.R. China; [2]Department of Clinical Laboratory, Zhejiang Hospital, Hangzhou, Zhejiang 310013, P.R. China

Received November 25, 2024; Accepted May 12, 2025

DOI: 10.3892/ijmm.2025.5563

Abstract. Psoriasis, the most common inflammatory skin disease, is marked by excessive proliferation of keratinocytes and infiltration of immune cells into the epidermis. Current treatments, particularly biologics targeting the IL-23/IL-17 axis, demonstrate excellent efficacy, but issues of recurrence and side effects persist. Therefore, it is essential to identify safer and more effective alternatives. Lobetyolin (LBT), a key component of polyacetylenes in *Codonopsis pilosula*, exhibits potent antioxidant and antitumor properties, yet its potential for treating psoriasis remains unexplored. In the present study, it was found that topical treatment with LBT significantly inhibits psoriasis in mice and maintains skin homeostasis during disease progression by regulating genes associated with keratinocyte proliferation and differentiation, enhancing the PPAR signaling pathway, and upregulating genes and metabolites involved in linoleic acid metabolism. Additionally, LBT suppressed gene expression linked to cytokine activity as well as the *Il17*, *Tnf* and MAPK signaling pathways in IMQ-treated dendritic cells (DCs). These findings underscored LBT's efficacy in reducing IMQ-induced psoriasis-like skin inflammation by preserving skin homeostasis and inhibiting inflammatory cytokines in DCs. The present results suggested that topically applied LBT could serve as a promising drug candidate for psoriasis treatment or as an adjunct to biologic therapies to prevent disease relapse.

Correspondence to: Dr Jie Zhu, Department of Clinical Laboratory, Zhejiang Hospital, 12 Lingying Road, Hangzhou, Zhejiang 310013, P.R. China
E-mail: dawnnyzj@aliyun.com

Dr Jiang Zhu, Department of Dermatology and Venereology, Sir Run Run Shaw Hospital, Zhejiang University School of Medicine, 3 Qingchun Road, Hangzhou, Zhejiang 310016, P.R. China
E-mail: zhujiang1@zju.edu.cn

*Contributed equally

Key words: lobetyolin, psoriasis, skin homeostasis, linoleic acid metabolism, inflammatory cytokines, dendritic cells

Introduction

Psoriasis is a chronic autoimmune skin condition characterized by the aberrant interaction between hyperproliferative keratinocytes and activated immune cells, leading to the formation of scales and red patches which substantial negative effects on patient quality of life (1). However, the underlying mechanisms of aberrant keratinocytes and activated immune cells in psoriasis are incompletely understood. Although current treatments include topical treatments, phototherapy, systemic treatments and biologics, there is no complete cure for psoriasis (2). Further research is recommended to investigate novel druggable targets that could enhance treatment outcomes for psoriasis.

Dendritic cells (DCs) play an important role in the initiation of psoriasis due to their ability to identify and present self-nucleotides that emerge from cellular distress, subsequently leading to T cell activation and proliferation (3). DCs produce interleukin (IL)-23, IL-12, tumor necrosis factor-α (TNF-α), and various other cytokines that significantly enhance the differentiation of naive T cells into Th (T help)1, Th17, and Th22 subsets. IL-23 plays a crucial role in sustaining and promoting the proliferation of pathogenic Th17 cells (4). Biological therapies targeting the IL-23/IL-17 axis are approved for clinical use and show excellent efficacy (5,6). However, the recurrence of psoriasis may still occur following the administration of IL-23 inhibitors, such as ustekinumab and guselkumab (7,8). Additionally, side effects associated with IL-23 inhibitors have been linked to an increased risk of infections, as evidenced by clinical trials and post-marketing surveillance (1,9). Therefore, it is necessary to find safer and more effective drugs to inhibit the production of inflammatory factors in DCs.

Lobetyolin (LBT; PubChem CID: 14655097) is a bioactive compound extracted from *Codonopsis pilosula* (*C. pilosula*), commonly known as Dangshen in Chinese (10). There is increasing evidence suggesting that LBT possesses anti-inflammatory, anti-oxidative, and xanthine oxidase

inhibiting properties (11,12). For example, LBT significantly reduced serum levels of IL-6, TNF-α and IL-1β while inhibiting inflammatory cell infiltration in lung and liver tissues during LPS-induced sepsis (13). Additionally, LBT protects BV2 microglial cells from oxygen-glucose deprivation/reperfusion damage by regulating their phenotypic polarization and reducing inflammatory responses, specifically by suppressing the production of TNF-α, IL-6, inducible nitric oxide synthase and CD206 (14). However, its potential impact on regulating DCs activation and psoriasis remains unknown.

The present study revealed new insights into LBT's role in Imiquimod (IMQ)-induced psoriasis-like inflammation. Our findings showed that LBT notably inhibited psoriasis in mice and helped maintain skin homeostasis during its progression by regulating the expression of genes related to keratinocyte proliferation and differentiation, enhancing the peroxisome proliferator-activated receptors' (PPAR) signaling pathway, and upregulating genes and metabolites involved in linoleic acid metabolism. Moreover, LBT inhibited gene expression linked to cytokine activity, as well as the IL-17, TNF, and mitogen-activated protein kinase (MAPK) signaling pathways in IMQ-treated DCs. These results highlighted LBT's significant ability to reduce IMQ-induced psoriasis-like skin inflammation by maintaining skin homeostasis and suppressing inflammatory cytokines in DCs, indicating its potential as a therapeutic agent for psoriasis.

Materials and methods

Reagents and mice. LBT (HY-N0327) was procured from MedChemExpress. IMQ (cat. no. tlrl-imq-1) was acquired from InvivoGen. Recombinant mouse GM-CSF (cat. no. 315-03) was sourced from PeproTech, Inc. APC-CD45 (cat. no. 109814) antibody was sourced from BioLegend, Inc. RPMI-1640 medium, along with penicillin, streptomycin, and fetal bovine serum, were obtained from Gibco-BRL (Thermo Fisher Scientific, Inc.). TRIzol® reagent was supplied by Invitrogen; Thermo Fisher Scientific, Inc. The ReverTra Ace qPCR RT Kit (cat. no. FSQ-201) was purchased from Toyobo Life Science, while the SYBR Green master Rox (cat. no. 04707516001) was obtained from Roche. Anti-mouse IL-23 (p19) antibody (cat. no. 513807) was purchased from BioLegend, Inc. KRT 6A antibody (cat. no. 10590-1-AP) was purchased from Proteintech Group, Inc.

Male C57BL/6 mice (8 weeks-old, average weight, 22 g) were obtained from the Shanghai SLAC Laboratory Animal Center and housed at the Zhejiang University Laboratory Animal Center with specific pathogen-free conditions, maintained on a 12/12-h light-dark cycle with lights activated at 8:00 a.m., in a controlled environment (23±1˚C, 60±5% humidity) with *ad libitum* access to standard rodent chow and autoclaved water. All animal experiments were conducted in accordance with relevant guidelines and regulations approved by the Institutional Animal Care and Use Committee at Zhejiang University. The present study received approval (approval no. 20220283) from the Ethics Committee of Zhejiang University School of Medicine (Hangzhou, China).

IMQ induced psoriasis-like skin inflammation in the mice model. A cohort of 196 8-week-old male C57BL/6 mice (initial n=52, expanded to 196 during revision) were randomized into eight experimental groups: PBS control, 1 mM LBT, 10 mM LBT, IMQ alone, IMQ + PBS, IMQ + 1 mM LBT, IMQ + 10 mM LBT, and IMQ + anti-IL-23p19 antibody (100 μg, i.p.). Psoriasis was induced by daily topical application of 62.5 mg 5% IMQ cream (Aldara®) on shaved dorsal/auricular skin for 5 consecutive days, with LBT treatments (1 mM or 10 mM in PBS) applied topically twice daily. The IMQ challenge elicited characteristic psoriasiform dermatitis including erythema, edema, epidermal hyperplasia and scaling. Strict humane endpoints were enforced, requiring euthanasia by pentobarbital sodium overdose (50 mg/kg, i.p.) followed by cervical dislocation for mice exhibiting ≥20% weight loss, cachexia, prolonged feeding impairment, or mobility deficits. The cessation of breathing and heartbeat for more than 2 min post-euthanasia was continuously observed prior to tissue collection. Throughout the 6-day study period, all animals underwent at least twice daily (morning and evening) health and behavioral monitoring to assess disease progression and treatment efficacy.

Histological analysis. Mouse back skin or ear tissues were fixed in 4% formaldehyde at 20-25˚C (room temperature) for 48 h for proper tissue fixation. The fixed tissues then underwent dehydration through a series of alcohol solutions with increasing concentrations from 75-100%. Next, the tissues were embedded in wax and sliced into ~5-μm thick sections. After blanching in hot water, the sections were affixed to glass slides and dried in a controlled environment at 45˚C. Before staining, the wax was removed using xylene, followed by sequential immersion in decreasing concentrations of alcohol and rinsing with distilled water. The slices were dehydrated in 70 and 90% alcohol for 10 min each, then stained with an alcohol-eosin solution for 2 to 3 min. Lastly, the stained sections were dehydrated in pure alcohol and rendered transparent with xylene prior to microscopic examination. Ki67 staining was performed using anti-Ki67 (Clone SP6; cat. no. ab16667; Abcam) at 1:200 dilution, incubated overnight at 4˚C, followed by DAB visualization. Stained sections were observed using a light microscope (IX73; Olympus Corporation). The epidermal thickness of the skin was calculated as the area of epidermis/the length of epidermis.

Flow cytometry analysis. Single cells from the ear were isolated following a previously published protocol (15). The cells were then collected and processed to obtain a single-cell suspension, with removal of cell clumps and debris. Subsequently, the suspension was centrifuged and resuspended in a flow cytometry staining solution for staining with APC-CD45 antibodies (1:200 dilution), followed by analysis using a BD Fortessa Cell Analyzer (BD Biosciences). The resulting data were analyzed using FlowJo v10.6.2 software (FlowJo LLC).

RNA-Seq detects the differentially expressed genes (DEGs). Total RNA was isolated using TRIzol™ Reagent (cat. no. 15596026; Thermo Fisher Scientific, Inc.) according to the manufacturer's protocol. RNA quantity and integrity were assessed using the Qubit™ 3.0 Fluorometer (cat. no. Q33216;

Thermo Fisher Scientific, Inc.) and Agilent 5300 Fragment Analyzer System (cat. no. M5310AA; Agilent Technologies) respectively. RNA samples demonstrating high purity (A260/A280 ratio 1.8-2.2) and RNA integrity numbers >7.0 were selected for subsequent library preparation using Illumina-compatible protocols. mRNA was purified from 2 μg total RNA using mRNA Capture Beads 2.0 (cat. no. 12629ES; Shanghai Yeasen Biotechnology Co., Ltd.) through two rounds of poly(A) selection.

Purified mRNA was fragmented in magnesium-containing fragmentation buffer (cat. no. 12340ES97; Shanghai Yeasen Biotechnology Co., Ltd.) at 94˚C for 5 min. First-strand cDNA was synthesized using random hexamer-primed reverse transcription (SuperScript™ IV Reverse Transcriptase; Thermo Fisher Scientific, Inc.). Second-strand cDNA was generated using a dUTP incorporation strategy with E. coli DNA Polymerase I, RNase H, and dUTP solution (cat. no. 12340ES97; Shanghai Yeasen Biotechnology Co., Ltd.). Blunt-ended cDNA fragments were adenylated at 3' ends using Klenow Fragment (3'→5' exo-) and ligated to Illumina-compatible forked adapters (IDT) containing T-overhangs. PCR products were size-selected (400±50 bp inserts) using Hieff NGS DNA Selection Beads (cat. no. 12601ES75; Shanghai Yeasen Biotechnology Co., Ltd.). Strand specificity was maintained through dUTP-based strand marking and uracil excision. Libraries were sequenced in 2x150 bp paired-end mode on an Illumina NovaSeq™ X Plus platform (LC-bio Technologies Hangzhou, Co., Ltd.) following manufacturer-recommended protocols.

Differential expression analysis of genes was performed by DESeq2 software (https://bioconductor.org/packages/release/bioc/html/DESeq2.html) between two different groups (and by edgeR between two samples). The genes with the parameter of false discovery rate (FDR) below 0.05 and absolute fold change ≥2 were considered DEGs. DEGs were then subjected to enrichment analysis of Gene Ontology (GO) functions and Kyoto Encyclopedia of Genes and Genomes (KEGG) pathways.

RNA isolation and reverse transcription-quantitative PCR (RT-qPCR). Total RNA was extracted from skin tissue or DCs using TRIzol reagent (Takara Biotechnology Co., Ltd.) according to the manufacturer's instructions. Reverse transcription was performed with the HiScript III 1st Strand cDNA Synthesis Kit (+gDNA wiper) (cat. no. R312-01; Vazyme Biotech Co., Ltd.) according to the manufacturer's instructions. RT-qPCR was conducted using SYBR Green Master Mix, and the relative difference was expressed as the fold change compared with control values, calculated using the comparative cycle method ($2^{-\Delta\Delta Cq}$) (16). The PCR protocol begins with an initial denaturation at 95˚C for 5 min, followed by 35 cycles of amplification, each consisting of denaturation at 95˚C for 10 sec and a combined annealing/extension step at 60˚C for 30 sec. After cycling, a melt curve analysis performed by heating to 95˚C for 15 sec, cooling to 60˚C for 1 min, and then gradually ramping to 95˚C to assess amplicon specificity. *Actb* gene was used as an internal control to normalize the expression of the target genes across experimental samples. The primer sequences are listed in Table SI.

Non-targeted metabolomics profiling analysis. Back-skin tissues from mice treated with IMQ or LBT were collected and analyzed at Hangzhou Lianchuan Biotechnology Co. Skin tissue samples (25±1 mg) were collected, mixed with beads and 500 μl of extraction solution (methanol: acetonitrile: water, 2:2:1 v/v) containing deuterated internal standards. The mixture was vortexed for 30 sec. The samples were incubated at -40˚C for 1 h to precipitate proteins. Subsequently, the samples were centrifuged at 12,000 rpm (RCF=13,800 x g, rotor radius=8.6 cm) for 15 min at 4˚C. The supernatant was transferred to fresh glass vials for analysis. Quality control (QC) samples were prepared by pooling equal volumes of the supernatants from all biological replicates.

LC-MS/MS analyses were performed using an UHPLC system (Vanquish; Thermo Fisher Scientific, Inc.) coupled with a Waters ACQUITY UPLC BEH Amide column (2.1x50 mm, 1.7 μm) and an Orbitrap Exploris 120 mass spectrometer (Thermo Fisher Scientific, Inc.). The mobile phase consisted of two solvents: A (25 mM ammonium acetate and 25 mM ammonia hydroxide in water, pH 9.75) and B (acetonitrile). The auto-sampler temperature was maintained at 4˚C, and the injection volume was 2 μl. The Orbitrap Exploris 120 mass spectrometer was operated in information-dependent acquisition (IDA) mode using Xcalibur software (Thermo Fisher Scientific, Inc.). In this mode, the acquisition software continuously evaluates the full scan MS spectrum to select precursor ions for MS/MS fragmentation. The ESI source conditions were set as follows: sheath gas flow rate at 50 Arb, auxiliary gas flow rate at 15 Arb, capillary temperature at 320˚C, full MS resolution at 60,000, MS/MS resolution at 15,000, collision energy at stepped normalized collision energy (NCE) of 20/30/40, and spray voltage at 3.8 kV (positive mode) or -3.4 kV (negative mode).

The raw data were converted to the mzXML format using ProteoWizard and processed with an in-house program developed in R, utilizing XCMS for peak detection, extraction, alignment and integration. Subsequently, an in-house MS2 database (https://www.tidymass.org/metid/articles/metabolite_annotation_using_MS2.html) was employed for metabolite annotation. The annotation cutoff was set at 0.3. The acquired MS data pretreatments including peak picking, peak grouping, retention time correction, second peak grouping, and annotation of isotopes and adducts was performed using XCMS software. The online KEGG, HMDB database was used to annotate the metabolites by matching the exact molecular mass data (m/z) of samples with those from database. Statistical analysis was performed in R (version 4.0.0) (17). Hypergeometric-based enrichment analysis with KEGG Pathway was performed to annotate protein sequences. The software Gene Set Enrichment Analysis (GSEA; v4.1.0) and MSigDB (https://www.gsea-msigdb.org/gsea/index.jsp) were used for gene set enrichment analysis to determine whether a set of genes in a specific KEGG pathway in different situations. Meeting this condition |NES|>1, NOM p-val<0.05, FDR q-val<0.25 were considered to be significantly different between the two groups.

BMDCs culture and treatments. Bone marrow cells were isolated from mice and cultured in RPMI-1640 medium supplemented with 10% FBS and 20 ng/ml GM-CSF. On

day 3, fresh medium with 20 ng/ml GM-CSF was added, and on day 5, half of the medium was replaced with fresh medium containing 20 ng/ml GM-CSF. BMDCs were harvested on day 6. All cells were cultured at 37˚C in a 5% CO_2 atmosphere. Before stimulation with IMQ (10 μg/ml) for 3 h, cells were pre-treated with 10 μM LTB for 24 h, as previously reported (13).

Enzyme linked immunosorbent assay (ELISA) assay. The Mouse IL-23 ELISA kit (cat. no. BMS6017; Thermo Fisher Scientific, Inc.) was used for detecting the level of IL-23 was performed according to the manufacturer's protocols. Briefly, 50 μl of cell supernatant was added to a plate coated with the capture antibody and incubated at room temperature for 2 h. Unbound antigens were washed away with TBST (0.05% Tween-20), followed by the addition of HRP-conjugated detection antibody and a further 1-h incubation at room temperature. Excess antibodies were then removed with TBST. Next, 50 μl of TMB chromogenic substrate was added and incubated for 15 min at room temperature. The reaction was stopped by adding 25 μl of sulfuric acid, and absorbance was measured at 450 nm.

Statistical analysis. All statistical analyses were conducted using GraphPad Prism 8 software (Dotmatics) and are presented as the mean ± SEM. Unpaired Student's t-test was used for comparisons between two groups, while two-way ANOVA followed by Tukey's honestly significant difference (HSD) post hoc test was utilized for comparisons involving more than two groups. $P<0.05$ was considered to indicate a statistically significant difference.

Results

LBT attenuates IMQ-induced psoriasis-like inflammation in mice. To assess LBT's effect on psoriasis-like skin inflammation, the IMQ cream was used to induce the psoriasis-like inflammation in mice. It was observed that IMQ significantly induced skin inflammation, characterized by pronounced immune cell infiltration, substantial keratinocyte proliferation, and thickening of the epithelial layer (Figs. S1A-C and 1A-F). Additionally, 1 or 10 mM LBT was applied to the dorsal skin and ears of mice treated with 5% IMQ cream for 5 days, and it was found that LBT significantly alleviated inflammatory symptoms (Fig. 1A). LBT-treated mice exhibited less inflammation, epidermal acanthosis, severe swelling, and keratinocyte proliferation compared with controls in back skin or ear (Fig. 1B-E). The proliferation marker Ki67 was also significantly reduced in the back skin of IMQ-induced psoriasis mice treated with LBT (Fig. 1F). Notably, LBT-treated mice showed less infiltration of $CD45^+$ immune cells post-IMQ treatment (Fig. 1G and H). Anti-mouse IL-23 (p19) antibody was used to treated IMQ-induced psoriasis-like inflammation. It was also observed LBT and the anti-IL-23 monoclonal antibody exhibited comparable therapeutic efficacy in suppressing psoriasis pathogenesis (Fig. 1A-H). These findings demonstrated that LBT effectively reduces IMQ induced psoriasis-like inflammation in mice.

LBT regulates the gene expression profile of extracellular region, keratinization and integral component of membrane in skin tissue of psoriasis mice. The gene expression profiles modulated by LBT were investigated in skin tissues from IMQ-induced psoriasis mice using RNA sequencing. Our analysis revealed that 978 genes were significantly upregulated, while 678 genes showed notable downregulation (Fig. 2A). GO functional enrichment analysis of all DEGs identified the top 20 dysregulated pathways (Fig. 2B). LBT notably regulated genes related to the extracellular region, keratinization and integral membrane components (Fig. 3B). Specifically, LBT significantly suppressed the expression of 113 genes associated with the extracellular region, including *Col12a1*, *Krt6a*, *Lrrc25*, *Lyn* and *Ccl2*, while it markedly upregulated 136 genes, such as *Card14*, *Mc5r* and *Oxtr* (Fig. 2C and D). LBT supplementation significantly upregulated 30 keratinization-related genes, including *Krt79*, *Lor*, *Lce1i*, *Lce1f* and *Lce1a2*, while downregulating 27 genes, such as *Sprr1b*, *Sprr2g*, *Krt6a* and *Krt16* (Fig. 2E and F). Additionally, LBT altered the expression of 336 integral membrane component genes, with 189 showing downregulation (Fig. 2G and H). Notably, the most significant changes occurred in *Slc7a11*, *Slc7a1*, *Ano9* and *Oxtr* (Fig. 2G and H). Given that hyperproliferation and abnormal differentiation of keratinocytes are hallmark features of psoriasis, it was confirmed that *Lce1c* and *Lor* expression significantly increased, whereas *Krt6a* and *Krt16* were significantly downregulated following LBT treatment in IMQ-induced inflammatory skin (Fig. 2I). Immunohistochemical analysis also revealed decreased KRT6A levels in the ear and back skin of IMQ-treated mice after LBT treatment (Fig. 2J). Overall, the results demonstrated that LBT regulates gene expression profiles related to the extracellular region, keratinization and integral membrane components.

KEGG analysis indicates that LBT regulates gene expression related to cytokine-cytokine receptor interactions and the PPAR signaling pathway in skin tissue of psoriasis mice. To investigate the effects of LBT on IMQ-induced psoriasis in mice, KEGG pathway enrichment analysis was conducted, revealing that LBT primarily influenced gene expression in neuroactive ligand-receptor interactions, cytokine-cytokine receptor interactions, and the PPAR signaling pathway, among others (Fig. 3A). Specifically, LBT upregulated 16 genes related to the PPAR signaling pathway, including *Acadm*, *Scd3*, *Slc27a4* and *Ppara*, while downregulating 3 genes, notably *Fads2* (Fig. 3B and C). LBT treatment resulted in the upregulation of 15 genes and a significant downregulation of 21 genes associated with cytokine-cytokine receptor interactions, with *Ccl12*, *Il33*, *Ccl2* and *Ccl4* being the most notably reduced (Fig. 3D and E). To further explore the mechanisms by which LBT influences psoriasis progression, GSEA analysis was employed to predict KEGG downstream pathways. The current findings indicated that LBT significantly activated the PPAR signaling pathway, while no significant effects were observed in the cytokine-cytokine receptor interaction pathway (Fig. 3F and G).

LBT could promote expression of the genes and metabolites related to linoleic metabolism in skin tissue of psoriasis mice. After using RNA-Seq to determine that LBT significantly

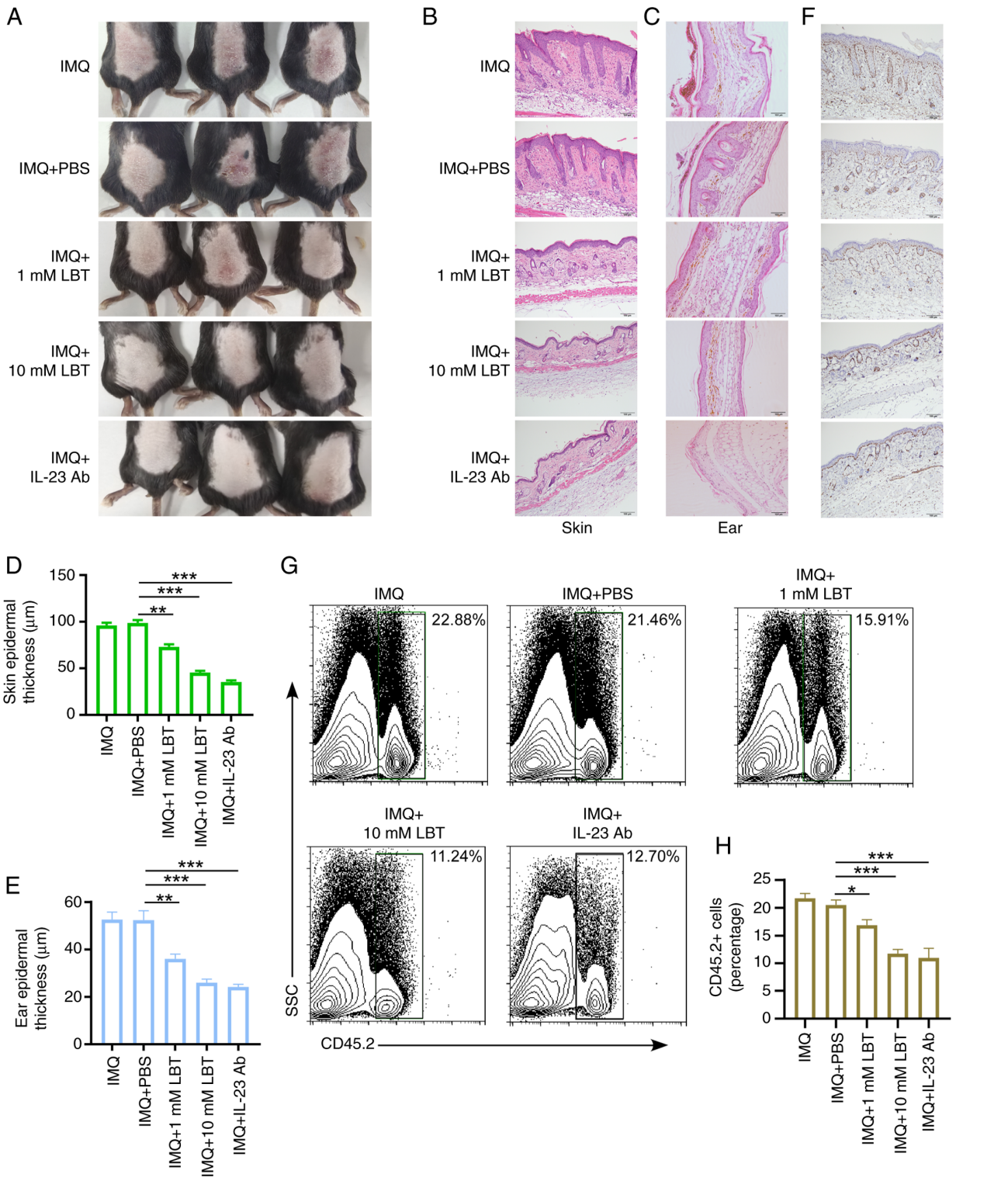

Figure 1. LBT attenuates IMQ-induced psoriasis-like inflammation in mice. C57BL/6 mice (n=6 per group) were subjected to daily topical application of IMQ cream on the shaved back or ear for five consecutive days, followed by topical administration of 1 or 10 mM LBT, PBS, or intraperitoneal injection of 100 μg anti-mouse IL-23 (p19) monoclonal antibody. (A) Representative images of dorsal back from mice (n=3/group). (B and C) H&E staining of (B) back skin and (C) ear skin sections obtained from IMQ-induced psoriatic mice treated with LBT or PBS for five days. (D and E) The epidermal thickness of the ears or skin was measured using ImageJ v1.8.0 software (National institutes of Health). (F) Immunohistochemical staining of Ki67 in back skin sections obtained from IMQ-induced psoriasis mice. (G and H) Flow cytometric analysis and statistical analysis of CD45$^+$ cells in the ears of mice. Scale bar, 100 μm. Data are representative of three independent experiments. P-values were determined by two-way ANOVA. *P<0.05, **P<0.01 and ***P<0.001. LBT, lobetyolin; IMQ, Imiquimod.

regulates metabolic gene expression, non-targeted metabolomics were conducted to assess metabolite changes. A total of 119 downregulated and 101 upregulated metabolites were identified (Fig. 4A). KEGG enrichment analysis indicated that LBT primarily affects arachidonic acid and linoleic acid metabolism (Fig. 4B). Additionally, linoleic acid levels

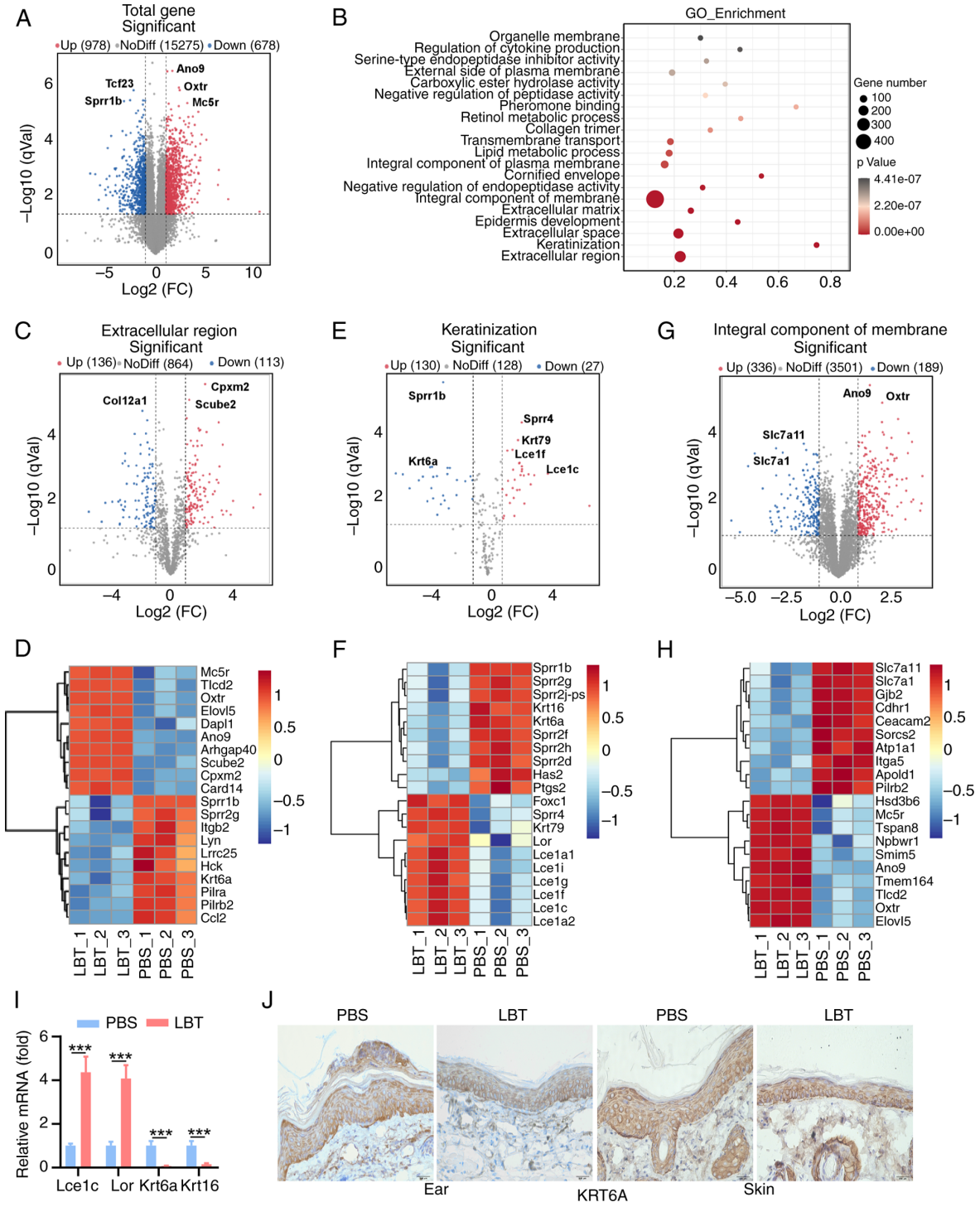

Figure 2. LBT regulates the gene expression profile of extracellular region, keratinization and integral component of membrane in skin tissue of psoriasis mice. The mRNAs were extracted from the back skin tissue of IMQ-induced psoriatic mice that had been treated with either LBT or PBS for a duration of five days. Subsequently, these samples were subjected to RNA sequencing. (A) Volcano plots showed all genes from the data obtained by RNA sequencing. (B) Scatter plot showed the top 20 most significantly changed GO terms. (C and D) Volcano plots identified the extracellular region (B), and the heat map highlighted the top 20 significantly altered DEGs with FPKM values >0 (C). (E and F) Volcano plots revealed (E) keratinization, and (F) the heat map showcased the top 20 significantly altered DEGs with FPKM values >0. (G and H) Volcano plots indicated the (G) integral component of the membrane, and (H) the heat map displayed the top 20 significantly altered DEGs with FPKM values >0. (I) Reverse transcription-quantitative PCR analysis detected *Lce1c*, *Lor*, *Krt6*a, *Krt16* mRNA level in the above back skin tissue. (J) Immunohistochemical staining of KRT6a in ear or back skin sections obtained from IMQ-induced psoriasis mice treated with 10 mM LBT or PBS for 5 days. Scale bar, 200 μm. Data are representative of three independent experiments. P-values were determined by two-way ANOVA. ***P<0.001. LBT, lobetyolin; IMQ, Imiquimod; DEGs, differentially expressed genes.

were significantly increased in IMQ-induced psoriasis mice following LBT treatment (Fig. 4C). RNA-Seq revealed that LBT upregulated seven genes, including *Cyp2j8*, *Cyp2j12* and *Cyp2e1*, while downregulating two genes (Fig. 4D and E). GSEA analysis showed that LBT significantly activated linoleic acid metabolism (Fig. 4F). Thus, the present findings

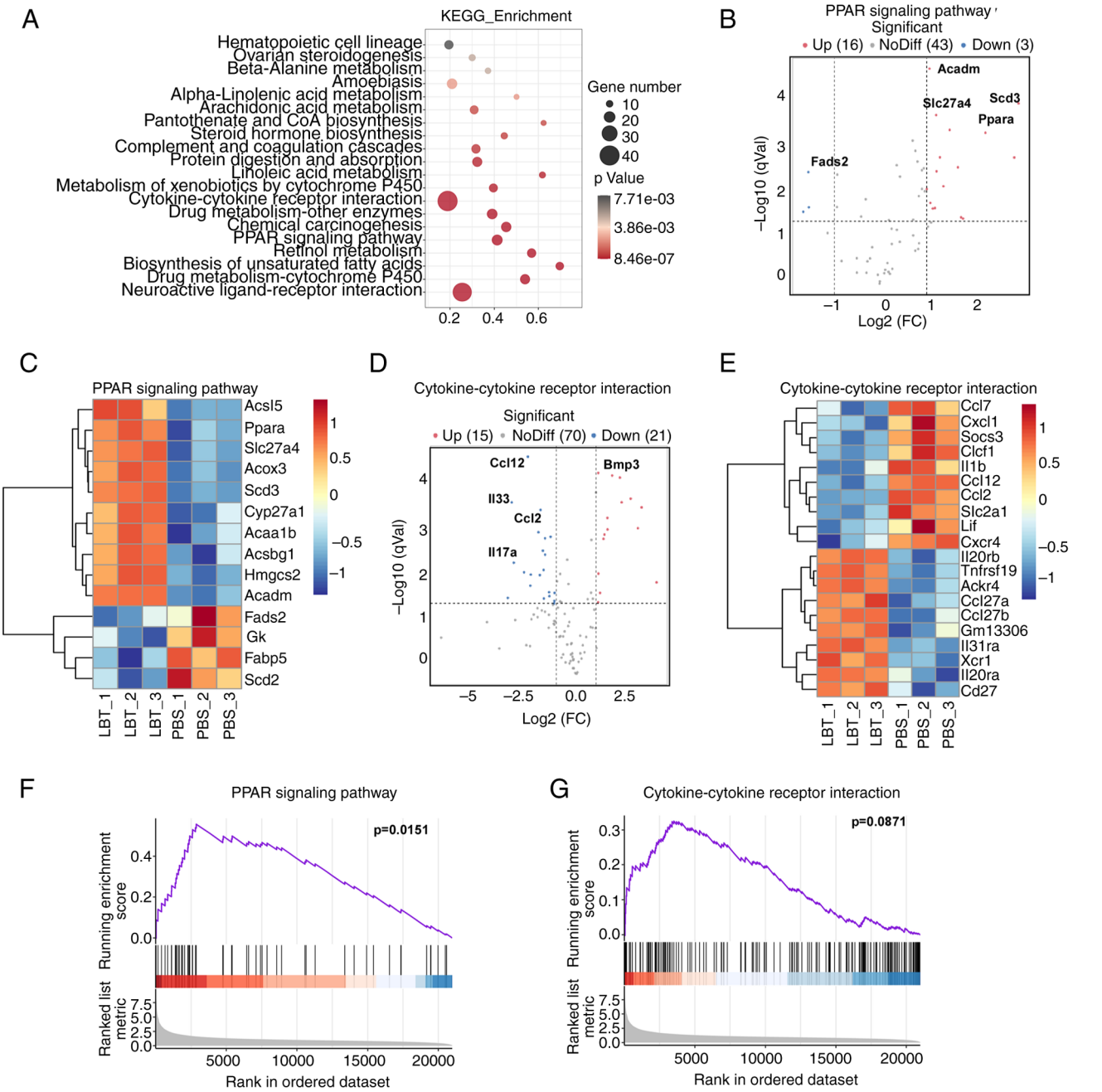

Figure 3. KEGG and GSEA analysis of DEGs regulated by LBT in skin tissue of Imiquimod-induced psoriasis mice. (A) Scatter plot showed the top 20 most significant KEGG pathways based on RNA-Seq data from the above back skin tissue. (B and C) Volcano plots and heat maps displayed significantly altered DEGs related to PPAR signaling pathway, all with FPKM values >0. (D and E) Volcano plots and heat maps revealed significantly altered DEGs related to cytokine-cytokine receptor interaction, all with FPKM values >0. (F and G) GSEA analysis of (F) PPAR signaling pathway and (G) cytokine-cytokine receptor interaction. KEGG, Kyoto Encyclopedia of Genes and Genomes; GSEA, Gene Set Enrichment Analysis; DEGs, differentially expressed genes; PPAR, peroxisome proliferator-activated receptors; FPKM, fragments per kilobase of transcript per million mapped reads.

demonstrated that LBT enhances linoleic acid metabolism by increasing the expression of associated genes.

LBT could inhibit expression of the genes related to cytokine activity, the IL-17, TNF and MAPK signaling pathways in IMQ-treated DCs. DCs play a vital role in the initiation and maintenance of psoriasis. The effects of LBT on peritoneal macrophages were analyzed after LPS stimulation using RNA-seq. Our results identified 201 DEGs in DCs treated with IMQ. Among these, 48 genes were markedly upregulated, while 153 were downregulated (Fig. 5A). KEGG pathway analysis indicated major alterations in the TNF signaling pathway, cytokine-cytokine interaction and IL-17 signaling pathway (Fig. 5B). GO analysis revealed considerable changes in cytokine-related genes in LBT-treated DCs under IMQ stimulation (Fig. 5C). Downregulation of14 genes linked to cytokine activity was observed, including *Il23a*, *Cxcl1*, and *Tnf* (Fig. 5D). Key genes in the TNF signaling pathway, such as *Jun*, *Tnf* and *Cxcl1*, were significantly downregulated in LBT-treated DCs after IMQ stimulation (Fig. 5E), alongside a reduction in MAPK signaling pathway genes including *Jun, Tnf* and *Dusp8* (Fig. 5F). To confirm the downregulation

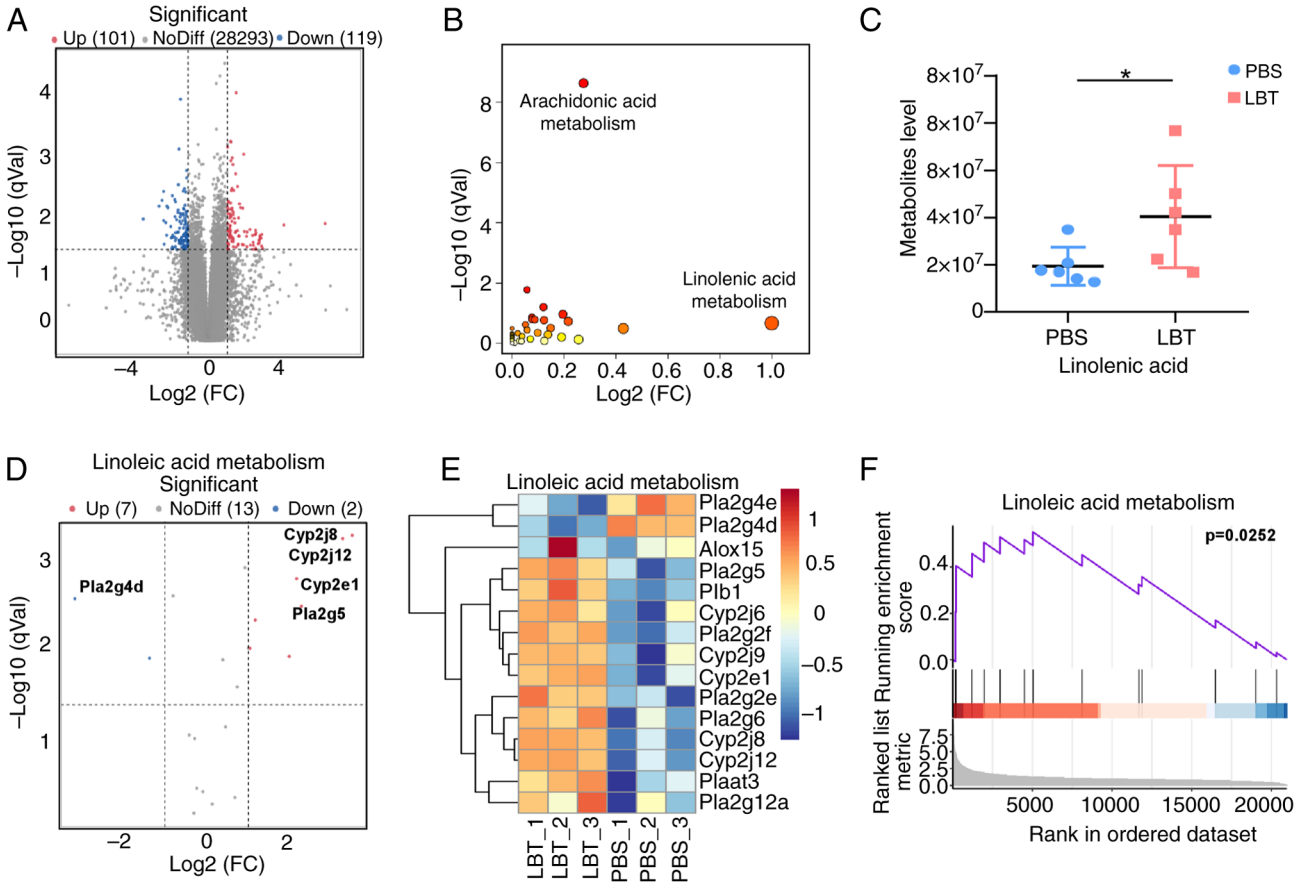

Figure 4. Non-targeted metabolomics and transcriptomics analysis in skin tissue of IMQ-induced psoriasis mice after treatment with LBT. (A) Volcano plots showed all metabolites from the data obtained by non-target metabolomics in skin tissues from IMQ-induced psoriasis mice treated with 10 mM LBT or PBS for 5 days. (B) Scatter plot for Kyoto Encyclopedia of Genes and Genomes analysis based on untargeted metabolism data. (C) The bar chart shows the level of linoleic acid detected by non-target metabolomics. (D and E) Volcano plots and heat maps revealed significantly altered differentially expressed genes related to linoleic acid metabolism, all with fragments per kilobase of transcript per million mapped reads values >0. (F) Gene Set Enrichment Analysis of linoleic acid metabolism based on the aforementioned RNA-Seq data from skin tissues. IMQ, Imiquimod; LBT, lobetyolin.

of genes in the IL-17, TNF and MAPK signaling pathways, RT-qPCR was performed, and it was found that the mRNA levels of *Il23*, *Tnf*, *Cxcl2*, *Il12b*, *Dusp1*, *Gadd45a*, *Nr4a1* and *Jun* were significantly reduced. Additionally, an ELISA assay indicated decreased IL-23A production in LBT-pre-treated DCs. These findings suggested that LBT effectively modulates gene expression related to cytokine activity, the IL-17, TNF and MAPK signaling pathways.

Discussion

Psoriasis is a common chronic inflammatory skin condition that significantly impacts individuals, healthcare systems and society (18). As the immunological mechanisms and pathogenesis of psoriasis are better understood, treatment options have greatly improved. Systemic agents targeting TNF-α, IL-17 and IL-23-such as infliximab, secukinumab and Ustekinumab-have shown effective and safe results (19,20). However, these treatments can cause severe side effects and often lead to disease recurrence after therapy ends. Therefore, it is crucial to develop strategies to prevent psoriasis recurrence post-treatment. LBT, derived from *Codonopsis pilosula*, has demonstrated cardioprotective, anti-inflammatory, antioxidant and antitumor effects (21). It protects mice from LPS-induced sepsis by downregulating pro-inflammatory cytokines such as TNF-α, IL-6 and IL-1β in macrophages (13). Additionally, LBT exhibits significant anticancer properties in gastric and breast cancer cells by inhibiting cell proliferation and inducing apoptosis through ASCT2 downregulation (22). It also shows notable cardioprotective and anti-arrhythmic activities (23). In the present study, it was found that LBT alleviates symptoms and regulates gene expression associated with keratinization, cytokine-receptor interactions, PPAR signaling and linoleic metabolism in mice with IMQ-induced psoriasis-like inflammation.

Psoriatic lesions feature epidermal acanthosis, hyperkeratosis and parakeratosis, resulting from increased keratinocyte proliferation and abnormal terminal differentiation (24). Keratins (KRTs), which form the intermediate filament network in epithelial cells, are essential for maintaining keratinocyte structural stability (25). Research indicates three KRTs associated with hyperproliferation in psoriatic epidermis: K6, K16 and K17 (26). Key epidermal barrier proteins, filaggrin and loricrin (LOR), show decreased expression in both lesional and non-lesional skin of psoriasis patients (27,28). The late cornified envelope (LCE) genes, located in the epidermal differentiation complex on chromosome1, encode18 largely function-unknown

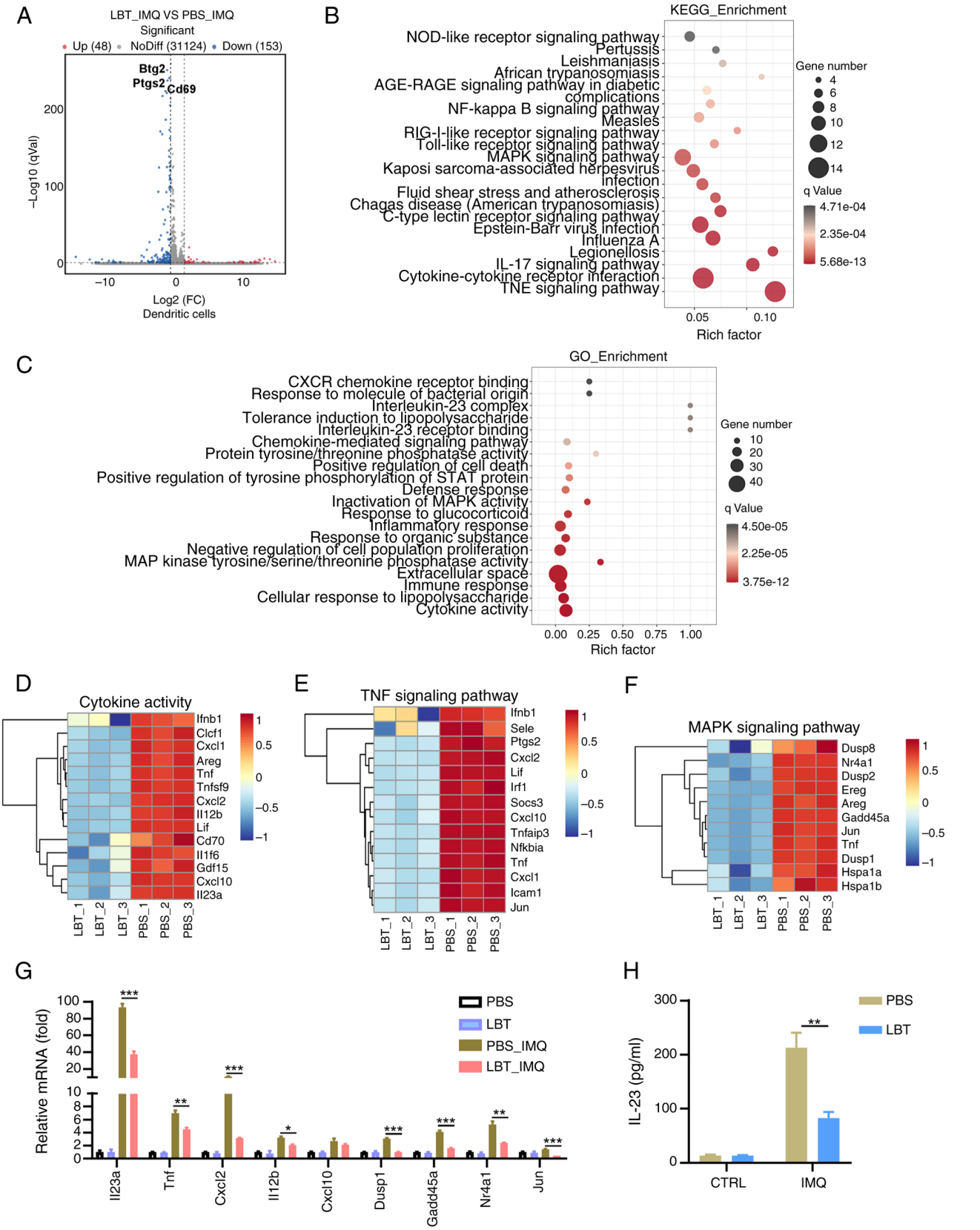

Figure 5. LBT could inhibit expression of the genes related to cytokine activity, IL-17 signaling pathway, TNF signaling pathway and MAPK signaling pathway in IMQ-treated DCs. The mRNAs were extracted from DCs treated with either LBT or PBS for 24 h, followed by stimulation with 10 μg/ml IMQ for 1 h, after which the samples underwent RNA sequencing. (A) Volcano plots showed all genes from the data obtained by RNA sequencing. (B and C) Scatter plot revealed the top 20 most significantly changed (B) KEGG and (C) GO terms. (D-F) Heat map displayed significantly changed differentially expressed genes related to (D) cytokine activity, (E) TNF signaling pathway and (F) MAPK signaling pathway. (G) Reverse transcription-quantitative PCR analysis detected the *Il23*, *Tnf*, *Cxcl2*, *Il-12b*, *Cxcl10*, *Dusp1*, *Gadd45a*, *Nr4a1* and *Jun* mRNA level in DCs treated with either LBT or PBS for 24 h, then stimulated with 10 mg/ml IMQ for 1 h. (H) ELISA analysis measured IL-23 levels in DCs treated with either LBT or PBS for 24 h, followed by 24-h stimulation with 10 μg/ml IMQ. Data are representative of three independent experiments. P-values were determined by two-way ANOVA. *P<0.05 **P<0.01 and ***P<0.001. LBT, lobetyolin; IMQ, Imiquimod; DCs, dendritic cells; KEGG, Kyoto Encyclopedia of Genes and Genomes; GO, Gene Ontology.

proteins, with the deletion of LCE3B and LCE3C being a well-established psoriasis risk factor linked to the major risk gene HLA-C*06 (29,30). All LCE groups (1,2,5, and 6) were significantly downregulated in psoriatic skin or IMQ-induced psoriasiform dermatitis mice (31). The current findings reveal increased expression of *Lce1c* and *Lor*, while *Krt6a* and *Krt16* were notably downregulated after LBT treatment. This suggests that LBT may regulate keratinocyte proliferation and differentiation. Further investigation is needed to explore LBT's role in keratinocytes.

Advancements in metabolomic and bioinformatic analyses have highlighted metabolism as a key factor in psoriasis pathogenesis. Various forms of cellular metabolism-such as glycolysis, the tricarboxylic acid cycle, lipid metabolism and amino acid metabolism-regulate keratinocytes and related immune cells (32). Lipid metabolism, particularly involving polyunsaturated fatty acids (PUFAs) like α-linolenic acid (ALA) and linoleic acid (LA), is crucial for both structural integrity and homeostasis in the stratum corneum, the outermost epidermal layer composed of corneocytes within a lipid matrix (33). LA is vital for skin barrier function as it is incorporated into ω-hydroxylated ceramides, which bind covalently to corneocytes and support lipid matrix organization (34). Dietary supplementation with ALA has been shown to reduce T cell signaling activation, thereby decreasing inflammatory cytokine secretion in psoriatic patients (35). Clinically, n-3 PUFAs are commonly used to alleviate psoriasis symptoms (36). Plasma samples from 56 psoriatic patients revealed significantly reduced total PUFAs, along with lower levels of α-linolenic acid (C18:3n3) and linoleic acid (C18:2n6) (37). This indicates that dysregulation of LA metabolism is closely linked to psoriasis onset. The present study demonstrated that LA levels and gene expression related to LA metabolism significantly increased after LBT treatment in the skin of IMQ-induced psoriasis mice, suggesting that LBT may modulate LA metabolism in the skin. Further research is necessary to explore LBT's effects on LA metabolism in keratinocytes.

Communication between immune cells and keratinocytes via cytokines and their receptors is crucial in psoriasis pathogenesis. Immune cells primarily produce cytokines including TNF-α, IFN-γ, IL-23/IL-17A and IL-22, which activate keratinocytes and initiate various signaling pathways, leading to excessive keratinocyte proliferation and the production of antimicrobial proteins, cytokines, chemokines and growth factors (38). Notably, TNF-α, IL-17A and IL-23 are central to psoriasis, as therapies targeting these cytokines are the most effective (39). In the present study, LBT treatment significantly downregulated the expression of *Il17a*, *Il1b*, *Ccl12*, *Il33*, *Ccl2* and *Ccl4* in the skin of IMQ-induced psoriasis mice. Additionally, a significant inhibition of *Il23a*, *Tnf* and *Cxcl2* gene expression was observed in DCs following IMQ treatment. Thus, the current findings indicated that LBT can modulate inflammatory cytokine production in DCs and mitigate psoriasis progression.

In the present study, it was also identified that LBT promotes the expression of genes associated with the PPAR signaling pathway. PPARs, comprising three subtypes (PPARα, PPARβ/δ and PPARγ), regulate genes involved in glucose and lipid metabolism, inflammation and differentiation (40). They are crucial for maintaining skin barrier permeability, inhibiting keratinocyte growth, promoting terminal differentiation, and regulating skin inflammation (41). For instance, activating PPAR-γ enhances cell differentiation, reduces proliferation, and modulates immune responses, alleviating inflammation in TNF-α-induced fibroblast-like synoviocytes in rheumatoid arthritis (42). PPAR-γ may regulate abnormal lipid metabolism, inflammatory cytokines and keratinocytes in psoriasis' pathogenesis (43), leading us to hypothesize that LBT may suppress psoriasis development by upregulating PPAR. Additionally, it was found that LBT significantly downregulated genes related to the MAPK signaling pathway, which plays a key role in psoriasis pathogenesis and regulating keratinocyte proliferation and immune responses (44). P38 and ERK1/2 are activated in psoriatic epidermis, and p38 activation leads to psoriasis-like dermatitis in mice, whereas ERK inhibition reduces IMQ-induced psoriasiform lesions (44,45). JNK/c-Jun signaling is necessary for the transcription of CCL2 and IL-23 in dendritic cells (46). In the present study, it was found that LBT could notably downregulate c-Jun expression, inhibiting IL-23 and TNF-α production.

Acknowledgements

The authors acknowledge the support from the Immunology Institute of Zhejiang University and the Public Technology Platform of Zhejiang University School of Medicine.

Funding

The present study was supported by the Natural Science Foundation of Zhejiang (grant no. LY22H110003).

Availability of data and materials

The data generated in the present study may be found in the Sequence Read Archive under accession number PRJNA1188620 or at the following URL: https://www.ncbi.nlm.nih.gov/sra/?term=PRJNA1188620 and in the Open Archive for Miscellaneous Data under accession number OMIX009890 or at the following URL: https://ngdc.cncb.ac.cn/omix/release/OMIX009890.

Authors' contributions

JP and JieZ conceived and designed the study. JH, CF, YX and SC performed the experiments. JiaZ, JC, HC, JP and YS analyzed the data. JH was a major contributor in writing the manuscript. JiaZ and JieZ assume overall responsibility for the manuscript. JieZ and JH confirm the authenticity of all the raw data. JZ was responsible for supervision and funding acquisition. All authors read and approved the final version of the manuscript.

Ethics approval and consent to participate

The present study was approved (approval no. 20220283) by the Ethics Committee of Zhejiang University School of Medicine (Hangzhou, China).

Patient consent for publication

Not applicable.

Competing interests

The authors declare that they have no competing interests.

References

1. Sieminska I, Pieniawska M and Grzywa TM: The immunology of psoriasis-current concepts in pathogenesis. Clin Rev Allergy Immunol 66: 164-191, 2024.
2. Ahmad A, Akhtar J, Ahmad M, Islam A, Badruddeen, Khan MI, Siddiqui S and Srivastava A: Curcumin nanogel preparations: A promising alternative for psoriasis treatment. Curr Drug Metab 25: 179-187, 2024.
3. Brunner SM, Ramspacher A, Rieser C, Leitner J, Heil H, Ablinger M, Tevini J, Wimmer M, Koller A, Piñón Hofbauer J, *et al*: Topical diacerein decreases skin and splenic $CD11c^+$ dendritic cells in psoriasis. Int J Mol Sci 24: 4324, 2023.
4. Song Y, Zhao X, Qu H, Su Y, He R, Chen L, Fang L, Li J, Zou Z, He J, *et al*: Epigenetic regulation of IL-23 by E3 ligase FBXW7 in dendritic cells is critical for psoriasis-like inflammation. J Immunol 211: 1701-1713, 2023.
5. Mohanakrishnan R, Beier S and Deodhar A: IL-23 inhibition for the treatment of psoriatic arthritis. Expert Opin Biol Ther 22: 59-65, 2022.
6. Fiechter RH, de Jong HM, van Mens LJJ, Fluri IA, Tas SW, Baeten DLP, Yeremenko NG and van de Sande MGH: IL-12p40/IL-23p40 blockade with ustekinumab decreases the synovial inflammatory infiltrate through modulation of multiple signaling pathways including MAPK-ERK and Wnt. Front Immunol 12: 611656, 2021.
7. Carmona-Rocha E and Puig L: The biological basis of disease recurrence in psoriasis. Ital J Dermatol Venerol 158: 279-291, 2023.
8. Bubna AK and Viplav V: Revisiting risankizumab: A newer biologic drug in dermatology. Ital J Dermatol Venerol 159: 543-554, 2024.
9. Megna M, Lauletta G, Tommasino N, Salsano A, Battista T, Ruggiero A, Martora F and Potestio L: Management of psoriasis patients with serious infectious diseases. Adv Ther 41: 2099-2111, 2024.
10. Feng YJ, Wang XX, Zhuang PY, Zhang DY, Gao L, Chen JM and Han G: Study on chemical constituents of *Codonopsis pilosula*. Zhongguo Zhong Yao Za Zhi 42: 135-139, 2017 (In Chinese).
11. Yue J, Xiao Y and Chen W: Insights into genus codonopsis: From past achievements to future perspectives. Crit Rev Anal Chem 54: 3345-3376, 2024.
12. Hu J, Wang D, Wang F and Lin P: Lobetyolin suppresses the proliferation of hepatocellular carcinoma through activating DUSP1-ERK1/2 signaling pathway. Biol Pharm Bull 47: 1751-1758, 2024.
13. Chen Z, Su Y, Ding J, He J, Lai L and Song Y: Lobetyolin protects mice against LPS-induced sepsis by downregulating the production of inflammatory cytokines in macrophage. Front Pharmacol 15: 1405163, 2024.
14. Wang J, Liu X, Wei W, Yang J, Li Q, Chu S, Liu P, Zhang J and He W: Regulation of oxygen-glucose deprivation/reperfusion-induced inflammatory responses and M1-M2 phenotype switch of BV2 microglia by lobetyolin. Metab Brain Dis 38: 2627-2644, 2023.
15. Yang W, He R, Qu H, Lian W, Xue Y, Wang T, Lin W, Zhu P, Xia M, Lai L and Wang Q: FXYD3 enhances IL-17A signaling to promote psoriasis by competitively binding TRAF3 in keratinocytes. Cell Mol Immunol 20: 292-304, 2023.
16. Livak KJ and Schmittgen TD: Analysis of relative gene expression data using real-time quantitative PCR and the 2(-Delta Delta C(T)) method. Methods 25: 402-408, 2001.
17. Domingo-Almenara X and Siuzdak G: Metabolomics data processing using XCMS. Methods Mol Biol 2104: 11-24, 2020.
18. Francis L, Capon F, Smith CH, Haniffa M and Mahil SK: Inflammatory memory in psoriasis: From remission to recurrence. J Allergy Clin Immunol 154: 42-50, 2024.
19. Katsiaunis A and Lipner SR: Devices for treatment of nail psoriasis. Ital J Dermatol Venerol 159: 561-565, 2024.
20. Mrowietz U, Lauffer F, Sondermann W, Gerdes S and Sewerin P: Psoriasis as a systemic disease. Dtsch Arztebl Int 121: 467-472, 2024.
21. Hou YY, Qi SM, Leng J, Shen Q, Tang S, Zhang JT, Hu JN, Jiang S and Li W: Lobetyolin, a Q-marker isolated from radix platycodi, exerts protective effects on cisplatin-induced cytotoxicity in HEK293 cells. J Nat Med 77: 721-734, 2023.
22. Bailly C: Anticancer properties of lobetyolin, an essential component of radix codonopsis (Dangshen). Nat Prod Bioprospect 11: 143-153, 2021.
23. Ni SH, OuYang XL, Liu X, Lin JH, Li Y, Sun SN, Deng JP, Han XW, Zhang XJ, Li H, *et al*: A molecular phenotypic screen reveals that lobetyolin alleviates cardiac dysfunction in 5/6 nephrectomized mice by inhibiting osteopontin. Phytomedicine 107: 154412, 2022.
24. Kouris A, Platsidaki E, Kouskoukis C and Christodoulou C: Psychological parameters of psoriasis. Psychiatriki 28: 54-59, 2017.
25. Cohen E, Johnson CN, Wasikowski R, Billi AC, Tsoi LC, Kahlenberg JM, Gudjonsson JE and Coulombe PA: Significance of stress keratin expression in normal and diseased epithelia. iScience 27: 108805, 2024.
26. Romashin DD, Tolstova TV, Varshaver AM, Kozhin PM, Rusanov AL and Luzgina NG: Keratins 6, 16, and 17 in health and disease: A summary of recent findings. Curr Issues Mol Biol 46: 8627-8641, 2024.
27. Kircik L, Alexis AF, Andriessen A, Blattner C, Glick BP, Lynde CW and Gold LS: Psoriasis and skin barrier dysfunction: The role of gentle cleansers and moisturizers in treating psoriasis. J Drugs Dermatol 22: 773-778, 2023.
28. Graubard R, Perez-Sanchez A and Katta R: Stress and skin: An overview of mind body therapies as a treatment strategy in dermatology. Dermatol Pract Concept 11: e2021091, 2021.
29. Niehues H, Tsoi LC, van der Krieken DA, Jansen PAM, Oortveld MAW, Rodijk-Olthuis D, van Vlijmen IMJJ, Hendriks WJAJ, Helder RW, Bouwstra JA, *et al*: Psoriasis-associated late cornified envelope (LCE) proteins have antibacterial activity. J Invest Dermatol 137: 2380-2388, 2017.
30. Coto E, Santos-Juanes J, Coto-Segura P, Díaz M, Soto J, Queiro R and Alvarez V: Mutation analysis of the LCE3B/LCE3C genes in psoriasis. BMC Med Genet 11: 45, 2010.
31. Utsunomiya A, Chino T, Utsunomiya N, Luong VH, Tokuriki A, Naganuma T, Arita M, Higashi K, Saito K, Suzuki N, *et al*: Homeostatic function of dermokine in the skin barrier and inflammation. J Invest Dermatol 140: 838-849.e9, 2020.
32. Solis ER and Jameson JM: Skin deep: Epithelial cell metabolism and chronic skin inflammation. Immunity 57: 1451-1453, 2024.
33. Simard M, Morin S, Ridha Z and Pouliot R: Current knowledge of the implication of lipid mediators in psoriasis. Front Immunol 13: 961107, 2022.
34. Simard M, Tremblay A, Morin S, Martin C, Julien P, Fradette J, Flamand N and Pouliot R: α-Linolenic acid and linoleic acid modulate the lipidome and the skin barrier of a tissue-engineered skin model. Acta Biomater 140: 261-274, 2022.
35. Hu X, Que W, Hirano H, Wang Z, Nozawa N, Ishii T, Ishizuka M, Ito H, Takahashi K, Nakajima M, *et al*: 5-Aminolevulinic acid/sodium ferrous citrate enhanced the antitumor effects of programmed cell death-ligand 1 blockade by regulation of exhausted T cell metabolism in a melanoma model. Cancer Sci 112: 2652-2663, 2021.
36. Kristensen S, Schmidt EB, Schlemmer A, Rasmussen C, Johansen MB and Christensen JH: Beneficial effect of n-3 polyunsaturated fatty acids on inflammation and analgesic use in psoriatic arthritis: A randomized, double blind, placebo-controlled trial. Scand J Rheumatol 47: 27-36, 2018.
37. Łuczaj W, Gęgotek A and Skrzydlewska E: Analytical approaches to assess metabolic changes in psoriasis. J Pharm Biomed Anal 205: 114359, 2021.
38. Kamata M and Tada Y: Crosstalk: Keratinocytes and immune cells in psoriasis. Front Immunol 14: 1286344, 2023.
39. Kim H, Choi MR, Jeon SH, Jang Y and Yang YD: Pathophysiological roles of ion channels in epidermal cells, immune cells, and sensory neurons in psoriasis. Int J Mol Sci 25: 2756, 2024.
40. Wagner N and Wagner KD: The role of PPARs in disease. Cells 9: 2367, 2020.
41. Wagner N and Wagner KD: Recent insights into the role of PPARs in disease. Cells 12: 1572, 2023.

42. Li XF, Yin SQ, Li H, Yang YL, Chen X, Song B, Wu S, Wu YY, Wang H and Li J: PPAR-γ alleviates the inflammatory response in TNF-α-induced fibroblast-like synoviocytes by binding to p53 in rheumatoid arthritis. Acta Pharmacol Sin 44: 454-464, 2023.
43. Lin X, Meng X, Song Z and Lin J: Peroxisome proliferator-activator receptor γ and psoriasis, molecular and cellular biochemistry. Mol Cell Biochem 477: 1905-1920, 2022.
44. An Y, Zhang Q, Ren Y, Yang S and Zhang Q: BML-111 modulates and alleviates p38/MAPK signaling pathway and Th1/Th2/Th17 cytokine response in murine psoriasis-like dermatitis. Discov Med 36: 2026-2036, 2024.
45. Long Q, Ma T, Wang Y, Chen S, Tang S, Wang T, Zhou Y, Xu K, Wan P and Cao Y: Orientin alleviates the inflammatory response in psoriasis like dermatitis in BALB/c mice by inhibiting the MAPK signaling pathway. Int Immunopharmacol 134: 112261, 2024.
46. Novoszel P, Holcmann M, Stulnig G, De Sa Fernandes C, Zyulina V, Borek I, Linder M, Bogusch A, Drobits B, Bauer T, *et al*: Psoriatic skin inflammation is promoted by c-Jun/AP-1-dependent CCL2 and IL-23 expression in dendritic cells. EMBO Mol Med 13: e12409, 2021.

Copyright © 2025 He et al. This work is licensed under a Creative Commons Attribution-NonCommercial-NoDerivatives 4.0 International (CC BY-NC-ND 4.0) License.